1 **Stable isotopic evidence for the excess leaching of unprocessed atmospheric**

2 **nitrate from forested catchments under high nitrogen saturation**

Weitian Ding[1], Urumu Tsunogai[1], Fumiko Nakagawa[1], Takashi Sambuichi[1], Masaaki

Chiwa[2], Tamao Kasahara[3], Ken'ichi Shinozuka[4]

[1]Graduate School of Environmental Studies, Nagoya University, Furo-cho, Chikusa-ku,

Nagoya 464-8601, Japan

[2]Kyushu University Forest, Kyushu University, Japan

[3]Faculty of Agriculture, Kyushu University, Japan

[4]River Basin Research Center, Gifu University, 1-1 Yanagido, Gifu, 501-1193, Japan

Corresponding author: Weitian Ding

Email: ding.weitian.v2@s.mail.nagoya-u.ac.jp

3 **Abstract**

4   Owing to the elevated loading of nitrogen through atmospheric deposition, some

5 forested ecosystems become nitrogen saturated, from which elevated levels of nitrate

6 are exported. The average concentration of stream nitrate eluted from upstream and

7 downstream of the Kasuya Research forested catchments (FK1 and FK2 catchments)

8 in Japan were more than 90 μM, implying that these forested catchments were under

9 nitrogen saturation. To verify that these forested catchments were under the nitrogen

10 saturation, we determined the export flux of unprocessed atmospheric nitrate relative to

11 the entire deposition flux (M_{atm}/D_{atm} ratio) in these catchments, because the M_{atm}/D_{atm}

12 ratio has recently been proposed as a reliable index to evaluate nitrogen saturation in

13 forested catchments. Specifically, we determined the temporal variation in the

14 concentrations and stable isotopic compositions, including $\Delta^{17}O$, of stream nitrate in

15 the FK catchments for more than 2 years. In addition, for comparison, the same

16 parameters were also monitored in the Shiiba Research forested catchment (MY

17 catchment) in Japan during the same period, where the average stream nitrate

18 concentration was low, less than 10 μM. While showing the average nitrate

19 concentrations of 109.5, 90.9, and 7.3 μM in FK1, FK2, and MY, respectively, the

20 catchments showed average $\Delta^{17}O$ values of +2.6, +1.5, and +0.6 ‰ in FK1, FK2, and

21 MY, respectively. Thus, the average concentration of unprocessed atmospheric nitrate

22 ($[NO_3^-{}_{atm}]$) was estimated to be 10.8, 5.1, and 0.2 μM in FK1, FK2, and MY,

23 respectively, and the M_{atm}/D_{atm} ratio was estimated to be 14.1, 6.6, and 1.3 % in FK1,

24 FK2, and MY, respectively. The estimated M_{atm}/D_{atm} ratio in FK1 (14.1 %) was the

25 highest ever reported from temperate forested catchments monitored for more than 1

26 year. Thus, we concluded that nitrogen saturation was responsible for the enrichment

27 of stream nitrate in the FK catchments, together with the elevated $NO_3^-{}_{atm}$ leaching

28 from the catchments. While the stream nitrate concentration ($[NO_3^-]$) can be affected

29 by the amount of precipitation, the M_{atm}/D_{atm} ratio is independent of the amount of

30 precipitation; thus, the M_{atm}/D_{atm} ratio can be used as a robust index for evaluating

31 nitrogen saturation in forested catchments.

33 **1 Introduction**

34 Nitrate is important as a nitrogenous nutrient in the biosphere. Traditionally, forested

35 ecosystems have been considered as nitrogen limited (Vitousek and Howarth, 1991).

36 However, owing to the elevated loading of nitrogen through atmospheric deposition,

37 some forested ecosystems become nitrogen saturated (Aber et al., 1989), from which

38 elevated levels of nitrate are exported (Mitchell et al., 1997; Peterjohn et al., 1996).

39 Such excessive leaching of nitrate from forested catchments degrades water quality and

40 causes eutrophication in downstream areas (Galloway et al., 2003; Paerl and Huisman,

41 2009). Thus, evaluating the stage of nitrogen saturation in each forested catchment

42 including its temporal variation, is critical for sustainable forest management,

43 especially for forested ecosystems under high nitrogen deposition.

44 Both concentration and seasonal variation of stream nitrate have been used as indexes

45 to evaluate the nitrogen saturation of each forested catchment in past studies (Aber,

46 1992; Rose et al., 2015; Stoddard, 1994). A forested stream eluted from Fernow

47 Experimental Forest USA, for instance, showed an elevated average nitrate

48 concentration of 60 μM, along with the absence of a seasonal variation in the stream

49 nitrate concentration, so the forest was classified into stage 3, the highest stage of

50 nitrogen saturation (Rose et al., 2015).

51   However, using both the concentration level (high or low) and seasonal variation

52 (clear or absent) of stream nitrate as indexes to evaluate nitrogen saturation has

53 limitations, including the following (1) seasonal variation of soil nitrate can be buffered

54 by groundwater with long residence time, so that the seasonal variation is unclear in

55 stream nitrate concentration in Japan, even in normal forests under the nitrogen

56 saturation stage of 0 (Mitchell et al., 1997); and (2) the stream nitrate concentration can

57 be enriched or diluted depending on the volume of rainfall, so the concentration level

58 can be high in low precipitation area irrespective of the stage of nitrogen saturation.

59   Nakagawa et al. (2018) lately proposed that the M_{atm}/D_{atm} ratio, the export flux of

60 unprocessed atmospheric nitrate (M_{atm}) relative to the deposition flux of $NO_3{}^-_{atm}$ (D_{atm}),

61 can be an alternative, more robust index for evaluating nitrogen saturation in each

62 forested catchment, because the M_{atm}/D_{atm} ratio directly reflects the demand for

63 atmospheric nitrate deposited onto each forested catchments as a whole, and thus reflect

64 the nitrogen saturation in each forested catchment. That is, we can expect high

65 M_{atm}/D_{atm} ratios in forested catchments under nitrogen saturation and low M_{atm}/D_{atm}

66   ratios in forested catchments with nitrogen deficiency.

67   To estimate the M_{atm}/D_{atm} ratio accurately and precisely in each forested catchment,

68   the fraction of unprocessed atmospheric nitrate ($NO_3^-{}_{atm}$) in the stream needs to be

69   estimated accurately and precisely. Triple oxygen isotopic compositions of nitrate

70   ($\Delta^{17}O$) have recently been used as a conservative tracer of $NO_3^-{}_{atm}$ deposited onto each

71   forested catchment (Inoue et al., 2021; Michalski et al., 2004; Nakagawa et al., 2018;

72   Tsunogai et al., 2014; Ding et al., 2022), showing distinctively different $\Delta^{17}O$ from that

73   of remineralized nitrate ($NO_3^-{}_{re}$), derived from organic nitrogen through general

74   chemical reactions, including microbial N mineralization and microbial nitrification.

75   While $NO_3^-{}_{re}$, the oxygen atoms of which are derived from either terrestrial O_2 or H_2O

76   through microbial processing (i.e., nitrification), always shows the relation close to the

77   "mass-dependent" relative relation between $^{17}O/^{16}O$ ratios and $^{18}O/^{16}O$ ratios; $NO_3^-{}_{atm}$

78   displays an anomalous enrichment in ^{17}O reflecting oxygen atom transfers from

79   atmospheric ozone (O_3) during the conversion of NO_X to $NO_3^-{}_{atm}$ (Alexander et al.,

80   2009; Michalski et al., 2003; Morin et al., 2011; Nelson et al., 2018). As a result, the

81     $\Delta^{17}O$ signature defined by the following equation (Kaiser et al., 2007) enables us to

82   distinguish $NO_3^-{}_{atm}$ ($\Delta^{17}O > 0$) from $NO_3^-{}_{re}$ ($\Delta^{17}O = 0$):

83
$$\Delta^{17}O = \frac{1 + \delta^{17}O}{(1 + \delta^{18}O)^{\beta}} - 1 \tag{1}$$

84   where the constant β is 0.5279 (Kaiser et al., 2007), $\delta^{18}O = R_{sample}/R_{standard} - 1$ and R is

85   the $^{18}O/^{16}O$ ratio (or the $^{17}O/^{16}O$ ratio in the case of $\delta^{17}O$ or the $^{15}N/^{14}N$ ratio in the case

86   of $\delta^{15}N$) of the sample and each standard reference material. In addition, $\Delta^{17}O$ is almost

87   stable during "mass-dependent" isotope fractionation processes within terrestrial

88   ecosystems. Therefore, while the $\delta^{15}N$ or $\delta^{18}O$ signature of $NO_3^-{}_{atm}$ can be overprinted

89   by the biological processes subsequent to deposition, $\Delta^{17}O$ can be used as a robust tracer

90   of unprocessed $NO_3^-{}_{atm}$ to reflect its accurate mole fraction within total NO_3^-,

91   regardless of the progress of the partial metabolism (partial removal of nitrate through

92   denitrification and assimilation) subsequent to deposition (Michalski et al., 2004;

93   Nakagawa et al., 2013, 2018; Tsunogai et al., 2011, 2014, 2018).

94   Past studies reported that the maximum concentration of stream nitrate was 58.4 μM

95   in the KJ forested catchment in Japan, with the maximum value of the M_{atm}/D_{atm} ratio

96   was 9.4 % (Nakagawa et al., 2018; Sase et al., 2022). Whether the index of the M_{atm}/D_{atm}

97   ratio can be applied to forested catchments, where the leaching of stream nitrate is much

98   higher than the KJ forested catchment, remained unclarified. Besides, the advantages

99   of the M_{atm}/D_{atm} ratio within the past indexes of nitrogen saturation have not been

100   discussed.

101   Chiwa (2021) has recently reported the enrichment of nitrate of more than 90 μM on

102   the annual average in forested streams eluted from the FK catchments (FK1 and FK2)

103   in Kasuya Research Forest, Kyushu University, Japan (Figs. 1a and 1b). The observed

104   enrichment of stream nitrate implied that these forested catchments were under nitrogen

105   saturation. Thus, in this study, we determined the M_{atm}/D_{atm} ratio in the FK1 and FK2

106   forested catchments by monitoring both the concentration and $\Delta^{17}O$ of stream nitrate

107   for more than 2 years to verify that these forested catchments were under nitrogen

108 saturation. For comparison, the MY forested catchment in Shiiba Research Forest,

109 Kyushu University, Japan (Figs. 1a and 1c), was also monitored during the same period,

110 where the average stream nitrate concentration was low (less than 10 µM). Furthermore,

111 the M_{atm}/D_{atm} ratios in these forested catchments were compared with those reported in

112 past studies to verify the reliability of the M_{atm}/D_{atm} ratio as an index of nitrogen

113 saturation.

114

115 **2 Methods**

116 2.1 Study sites

117 The FK forested catchments (33°38′N, 130°31′E) are located in a suburban area,

118 about 15 km west of the Fukuoka metropolitan area (the fourth largest metropolitan

119 area in Japan). The main plantation in these catchments was Japanese cedar/cypress

120 (Table 1). The MY forested catchment (32°22′N, 131°09′E) is located in a rural area at

121 the village of Shiiba in southern Japan's Central Kyushu Mountain range. This

122 catchment is a mixed forest consisting of coniferous trees such as *Abies firma Sieb. et*

123 *Zucc.,* and *Tsuga sieboldii Carr.,* and deciduous broadleaved trees such as *Quercus*

124 *crispula Blume*, *Fagus crenata Blume*, and *Acer sieboldianum* Miq. Details on the

125 studied forested catchments have been described in the past studies (Chiwa, 2020, 2021).

126

127 2.2 Sampling

128 The stream water eluted from the FK1 (14 ha), FK2 (62 ha), and MY (43 ha)

129 forested catchments were collected about once every month in principle from 2019/11

130 to 2021/12 (Fig. 1). At the FK catchments, stream water was collected at upstream

131 (station A) and downstream (station B) locations (Fig. 1b). At the MY catchment,

132 stream water was collected at station C (Fig. 1c). Samples of stream water to determine

133 the concentration and stable isotopic compositions ($\delta^{15}N$, $\delta^{18}O$, and $\Delta^{17}O$) of stream

134 nitrate were collected manually in bottles washed with deionized water before sampling

135 and then rinsed at least twice with the sample before sampling at each sampling site.

136

137 2.3 Analysis

138 All the stream water samples were passed through a membrane filter (pore size 0.45

139 µm) within two days after sampling and stored in a refrigerator (4 °C) until analysis.

140 The concentrations of nitrate were measured by ion chromatography (Prominence HIC-

141 SP, Shimadzu, Japan). To determine the stable isotopic compositions of nitrate in the

142 stream water samples, nitrate in each sample was chemically converted to N_2O using a

143 method originally developed to determine the $^{15}N/^{14}N$ and $^{18}O/^{16}O$ ratios of seawater

144 and freshwater nitrate (McIlvin and Altabet, 2005) that was later modified (Konno et

145 al., 2010; Tsunogai et al., 2011; Yamazaki et al., 2011). In brief, 11 mL of each sample

146 solution was pipetted into a vial with a septum cap. Then, 0.5 g of spongy cadmium

147 was added, followed by 150 µL of a 1 M $NaHCO_3$ solution. The sample was then shaken

148 for 18-24 h at a rate of 2 cycles s^{-1}. Then, the sample solution (10 mL) was decanted

149 into a different vial with a septum cap. After purging the solution using high-purity

150 helium, 0.4 mL of an azide–acetic acid buffer, which had also been purged using high-

151 purity helium, was added. After 45 min, the solution was alkalinized by adding 0.2 mL

152 of 6 M NaOH. Then, the stable isotopic compositions ($\delta^{15}N$, $\delta^{18}O$, and $\Delta^{17}O$) of the

153 N_2O in each vial were determined using the continuous-flow isotope ratio mass

154 spectrometry (CF-IRMS) system at Nagoya University. The analytical procedures

155 performed using the CF-IRMS system were the same as those detailed in previous

156 studies (Hirota et al., 2010; Komatsu et al., 2008a). The obtained values of $\delta^{15}N$, $\delta^{18}O$,

157 and $\Delta^{17}O$ for the N_2O derived from the nitrate in each sample were compared with those

158 derived from our local laboratory nitrate standards to calibrate the values of the sample

159 nitrate to an international scale and to correct for both isotope fractionation during the

160 chemical conversion to N_2O and the progress of oxygen isotope exchange between the

161 nitrate derived reaction intermediate and water (ca. 20 %). In this study, we adopted the

162 internal standard method to calibrate the stable isotopic compositions of sample nitrate.

163 Specifically, three kinds of the local laboratory nitrate standards were used in this study,

164 which were named to be GG01 ($\delta^{15}N$ = –3.07 ‰, $\delta^{18}O$ = +1.10 ‰, and $\Delta^{17}O$ = 0 ‰),

165 HDLW02 ($\delta^{15}N$ = +8.94 ‰, $\delta^{18}O$ = +24.07 ‰), and NF ($\Delta^{17}O$ = +19.16 ‰), which the

166 GG01 and the HDLW02 were used to determine the $\delta^{15}N$ and $\delta^{18}O$ of stream nitrate,

167 and the GG01 and the NF was used to determine the $\Delta^{17}O$ of stream nitrate. The GG01,

168 HDLW02, and NF had been calibrated using the internationally distributed isotope

169 reference materials (USGS 34 and USGS 35). The oxygen exchange rate between

170 nitrate and water during the chemical conversion was calculated through Eq. (2):

171   Oxygen exchange rate (%) = $\Delta^{17}O(N_2O)_{NF} / \Delta^{17}O(NO_3^-)_{NF}$ (2)

172   where the $\Delta^{17}O(N_2O)_{NF}$ denote the $\Delta^{17}O$ value of N_2O that convert from the NF

173   nitrate, the $\Delta^{17}O(NO_3^-)_{NF}$ denote the $\Delta^{17}O$ value of NF nitrate ($\Delta^{17}O$ = +19.16 ‰)

174   (Tsunogai et al., 2016; Nakagawa et al., 2013, 2018; Ding et al., 2022).

175   The δ^2H and $\delta^{18}O$ values of H_2O of the stream water samples were analyzed using

176   the cavity ring-down spectroscopy method by employing an L2120-i instrument

177   (Picarro Inc., Santa Clara, CA, USA) equipped with an A0211 vaporizer and

178   autosampler. The errors (standard errors of the mean) in this method were ±0.5‰ for

179   δ^2H and ±0.1‰ for $\delta^{18}O$. Both the VSMOW and standard light Antarctic precipitation

180   (SLAP) were used to calibrate the values to the international scale. The $\delta^{18}O$ values of

181   H_2O were used to calibrate the differences in $\delta^{18}O$ of H_2O between the samples and

182   those our local laboratory nitrate standard samples (Tsunogai et al., 2010, 2011, 2014).

183   To determine whether the conversion rate from nitrate to N_2O was sufficient, the

184   concentration of nitrate in the samples was determined each time we analyzed the

185   isotopic composition using CF-IRMS based on the N_2O^+ or O_2^+ outputs. We adopted

186   the $\delta^{15}N$, $\delta^{18}O$, and $\Delta^{17}O$ values only when the concentration measured via CF-IRMS

187   correlated with the concentration measured via ion chromatography prior to isotope

188   analysis within a difference of 10 %. We repeated the analysis of $\delta^{15}N$, $\delta^{18}O$, and $\Delta^{17}O$

189   values for each sample at least three times to attain high precision. All samples had a

190   nitrate concentration of greater than 3.5 μM, which corresponded to a nitrate quantity

191   greater than 35 nmol in a 10 mL sample. Thus, all isotope values presented in this study

192   have an error (standard error of the mean) better than ±0.2 ‰ for $\delta^{15}N$, ±0.3 ‰ for $\delta^{18}O$,

193   and ±0.1 ‰ for $\Delta^{17}O$.

194   Nitrite (NO_2^-) in the samples interferes with the final N_2O produced from nitrate

195   because the chemical method also converts NO_2^- to N_2O (McIlvin and Altabet, 2005).

196   Therefore, it is sometimes necessary to remove NO_2^- prior to converting nitrate to N_2O.

197   In this study, however, we skipped the processes for removing NO_2^- because all the

198   stream samples analyzed for stable isotopic composition had NO_2^- concentrations lower

199   than the detection limit (0.05 μM).

200

201   2.4 Deposition rate of atmospheric nitrate

202   The annual deposition rate of atmospheric nitrate (D_{atm}; total dry and wet deposition

203   rate of atmospheric nitrate) in each catchment was estimated using the annual "bulk"

204   deposition rate of atmospheric nitrate (D_{bulk}) calculated in Chiwa (2020) at each

205   catchment by multiplying the volume-weighted mean concentration of nitrate in the

206   bulk deposition samples collected every 2 weeks at each catchment for 10 years (from

207   2009/1 to 2018/12) by the annual amount of precipitation. The bulk deposition samples

208   were those accumulated in a plastic bucket installed in an open site of each catchment

209   55 cm above the ground. The distances between the monitoring sites of bulk deposition

210   in the FK1, FK2, and MY forested catchments and the stations of stream water sampling

211   (stations A, B, and C) were 3.9, 2.9, and 4.5 km, respectively. The concentrations of

212   nitrate in the bulk deposition samples were measured by ion chromatography.

213   The D_{bulk} determined through this method, however, is less than D_{atm} (Aikawa et al.,

214   2003) because the dry deposition velocities of gases and particles on the water surface

215   of the plastic bucket are smaller than those on the forest (Matsuda, 2008). Thus, we

216   corrected the differences by using Eq. (3) to estimate D_{atm} from D_{bulk}:

217      $D_{atm} = D_{bulk} - D_{dry}(W) + D_{dry}(F)$ (3)

218   where $D_{dry}(W)$ and $D_{dry}(F)$ denote the annual dry deposition rates onto water and forest,

219   respectively.

220   The $D_{dry}(W)$ and $D_{dry}(F)$ at each catchment were determined using an inferential

221   method (Endo et al., 2011) through Eqs. (4) and (5), respectively:

222      $D_{dry}(W) = [NO_3{}^-_{atm}]_{gas} \times V_{gas}(W) + [NO_3{}^-_{atm}]_p \times V_p(W)$ (4)

223      $D_{dry}(F) = [NO_3{}^-_{atm}]_{gas} \times V_{gas}(F) + [NO_3{}^-_{atm}]_p \times V_p(F)$ (5)

224   where $[NO_3{}^-_{atm}]_{gas}$ denotes the concentration of gaseous nitrate in air; $[NO_3{}^-_{atm}]_p$

225   denotes the concentration of particle nitrate in air; $V_{gas}(W)$ and $V_{gas}(F)$ denote the

226   deposition velocities of gaseous nitrate on the water surface and forest, respectively;

227   and $V_p(W)$ and $V_p(F)$ denote the deposition velocities of particulate nitrate on the water

228   surface and forest, respectively. Those determined by Chiwa (2010) using the annular

229   denuder method from 2006/5 to 2007/4 were used for the $[NO_3{}^-]_{gas}$ and $[NO_3{}^-]_p$ in the

230   FK catchments. Those determined by the National Institute for Environmental Studies

231   (Environmental Laboratories Association of Japan, 2017) using the filter-pack method

232   at Miyazaki (31°83′N, 131°42′E) from 2011 to 2017 were used for the $[NO_3{}^-]_{gas}$ and

233      $[NO_3{}^-]_p$ in the MY catchment. The $V_{gas}(F)$, $V_{gas}(W)$, $V_p(F)$, and $V_p(W)$ of each

234   catchment were determined by applying the estimation file for dry deposition (Matsuda,

235   2008;

236   http://www.hro.or.jp/list/environmental/research/ies/katsudo/acid_rain/kanseichinchak

237   u/kanseichinchaku.html), where V_{gas} and V_p were calculated using the meteorological

238   data of wind speed, temperature, humidity, radiation, and cloud amount and land use.

239   The meteorological data monitored by Japan Meteorological Agency at the nearest

240   Fukuoka station (33°34′N, 130°22′E) and Miyazaki station (31°56′N, 131°24′E) from

241   2009 to 2021 were used for the FK and MY catchments, respectively. The forested land

242   use of 100 % was chosen for each area.

243

244   2.5 Flux of stream water

245   The flux of stream water (F_{stream}) in each catchment was not measured fully in this

246   study. Instead, the water balance in each catchment was used to estimate F_{stream},

247   assuming that the outflux of water from the study catchments to deep groundwater was

248   negligible:

249    $F_{stream} = P - E$ (6)

250   where P denotes the annual average precipitation and E denotes the annual

251   evapotranspiration flux of water in each catchment. In this paper, the equation obtained

252   by Komatsu et al. (2008) was used to estimate the E of the FK and MY catchments.

253   Details on this equation are shown below.

254   Komatsu et al. (2008) compiled the annual flux of evapotranspiration determined in

255   43 forested catchments in Japan and found that E shows a positive correlation with the

256   average temperature (T_{avg}) of each catchment. Thus, they proposed the modeled relation

257   of E (mm) = 31.4T_{avg} (°C) + 376 to estimate E in each forested catchment in Japan,

258   where the standard error of 162.3 mm was included in the estimated evapotranspiration

259   flux (E). They also confirmed that the estimated F_{stream} using the model corresponded

260   well with the observed F_{stream} in three forested catchments, with estimated errors of less

261   than 6 %. As a result, we utilized the water balance method proposed by Komatsu et al.

262   (2008) to quantify the F_{stream} in each catchment.

263

264   2.6 Concentration of unprocessed $NO_3^-{}_{atm}$ in each water sample

265   The $\Delta^{17}O$ data of nitrate in each sample was used to estimate the concentration of

266     $NO_3^-{}_{atm}$ ([$NO_3^-{}_{atm}$]) in each water sample by applying Eq. (7):

267   [$NO_3^-{}_{atm}$]/[NO_3^-] = $\Delta^{17}O$/$\Delta^{17}O_{atm}$ (7)

268   where [$NO_3^-{}_{atm}$] and [NO_3^-] denote the concentrations of $NO_3^-{}_{atm}$ and nitrate (total) in

269   each water sample, respectively, and $\Delta^{17}O_{atm}$ and $\Delta^{17}O$ denote the $\Delta^{17}O$ values of

270     $NO_3^-{}_{atm}$ and nitrate (total) in the stream water sample, respectively. In this study, we

271   used the annual average $\Delta^{17}O$ value of $NO_3^-{}_{atm}$ determined at the Sado-Seki monitoring

272   station in Japan (Sado Island; Fig. 1a) from April 2009 to March 2012 ($\Delta^{17}O_{atm}$ =

273   +26.3 ‰; Tsunogai et al., 2016) for $\Delta^{17}O_{atm}$ in Eq. (7) to estimate [$NO_3^-{}_{atm}$] in the stream.

274   We allow for an error range of 3 ‰ in $\Delta^{17}O_{atm}$, where the factor changes in $\Delta^{17}O_{atm}$

275   from +26.3 ‰ caused by both areal and seasonal variations in the $\Delta^{17}O$ values of

$\text{NO}_3{}^-{}_{\text{atm}}$ have been considered (Nakagawa et al., 2018; Tsunogai et al., 2016; Ding et al., 2022).

The annual export flux of unprocessed $\text{NO}_3{}^-{}_{\text{atm}}$ per unit area of the catchment (M_{atm}) was determined by applying Eq. (8):

$$M_{\text{atm}} = [\text{NO}_3{}^-{}_{\text{atm}}]_{\text{avg}} \times F_{\text{stream}} \tag{8}$$

where $[\text{NO}_3{}^-{}_{\text{atm}}]_{\text{avg}}$ denotes the annual average $[\text{NO}_3{}^-{}_{\text{atm}}]$ in each stream. The index of nitrogen saturation ($M_{\text{atm}}/D_{\text{atm}}$ ratio) was calculated by dividing M_{atm} with D_{atm} in each catchment.

2.7 Concentration and isotopic compositions of stream nitrate eluted only from the FK2 catchment

The concentration and isotopic compositions ($\delta^{15}\text{N}$, $\delta^{18}\text{O}$, and $\Delta^{17}\text{O}$) of stream nitrate determined at ~~the~~ station B were the mixtures~~mixture~~ of those eluted from FK1 and FK2 catchments (Fig. 1b). Assuming that the stream nitrate eluted from FK1 catchment was stable during the flow path from station A to station B. The concentration of stream nitrate eluted from the FK2 catchment was determined by applying Eq. (9):

$$[\text{NO}_3{}^-]_{\text{FK2}} = ([\text{NO}_3{}^-]_{\text{FK1+FK2}} * F_{\text{FK1+FK2}} - [\text{NO}_3{}^-]_{\text{FK1}} * F_{\text{FK1}}) / F_{\text{FK2}} \tag{9}$$

where F_{FK1}, F_{FK2}, and $F_{\text{FK1+FK2}}$ denote the flux of stream water eluted from the FK1, FK2 (only), and FK1+FK2 catchment, respectively. $[\text{NO}_3{}^-]_{\text{FK1}}$, $[\text{NO}_3{}^-]_{\text{FK2}}$, and $[\text{NO}_3{}^-]_{\text{FK1+FK2}}$ denote the concentration of stream nitrate eluted from the FK1, FK2 (only), and FK1+FK2 catchment, respectively. In this study, the flow rates measured at

stations A and B on 2021/01/15 by using the salt dilution method (Sappa et al., 2015) was used for F_{FK1} (0.85 L/s) and $F_{FK1+FK2}$ (4.75 L/s), respectively, and the measured $[NO_3^-]$ at stations A and B was used for $[NO_3^-]_{FK1}$ and $[NO_3^-]_{FK1+FK2}$, respectively. Because the relation between the measured flow rates was comparable with the relation between the catchment area of FK1 (14 ha) and that of FK1+FK2 (76 ha), we concluded that the measured flow rates of 0.85 L/s and 4.75 L/s were reasonable as for those representing the F_{FK1} and $F_{FK1+FK2}$, respectively. According to the mass balance of water, we can estimate the F_{FK2} eluted from the FK2 catchment only to be 3.90 L/s.

Assuming that the stream nitrate eluted from FK1 catchment was stable during the flow path from station A to station B, the $\delta^{15}N$, $\delta^{18}O$, and $\Delta^{17}O$ values of stream nitrate eluted from the FK2 catchment only were determined by applying Eq. (10):

$$\delta_{FK2} = (\delta_{FK1+FK2} * [NO_3^-]_{FK1+FK2} * F_{FK1+FK2} - \delta_{FK1} * [NO_3^-]_{FK1} * F_{FK1}) / ([NO_3^-]_{FK2} * F_{FK2})$$

(10)

where δ_{FK1}, δ_{FK2}, and $\delta_{FK1+FK2}$ denote the $\delta^{15}N$ (or $\delta^{18}O$ or $\Delta^{17}O$) of stream nitrate eluted from the FK1, FK2, and FK1+FK2 catchment, respectively. The $\delta^{15}N$ (or $\delta^{18}O$ or $\Delta^{17}O$) values of stream nitrate measured at stations A and B were used for δ_{FK1} and $\delta_{FK1+FK2}$, respectively.

3 Results

3.1 Deposition rate of atmospheric nitrate

The mean annual precipitation (P) from 2009 to 2021 was 1777 mm and 3981 mm

for FK and MY catchments, respectively (Chiwa, 2020; Chiwa, personal

communication, September 21, 2022). The mean annual temperature (T_{avg}) was

reported to be 15.9 °C and 10.8 °C for FK and MY catchments, respectively (Chiwa,

2020). Based on these data, the annual flux of stream water (F_{stream}) was estimated to

be 902.0 ± 162.3 mm at FK catchments and 3266.1 ± 162.3 mm at MY catchment,

respectively, using Eq. (6).

Chiwa (2020) reported the annual bulk deposition rates of atmospheric nitrate (D_{bulk})

to be 34.0 mmol m^{-2} year^{-1} at FK catchments and 24.2 mmol m^{-2} year^{-1} at MY

catchment. On the other hand, the annual dry deposition rate of atmospheric nitrate

(D_{dry}) deposited on the forest (D_{dry}(F)) and on the water surface (D_{dry}(W)) were

estimated to be 39.9 mmol m^{-2} year^{-1} and 4.1 mmol m^{-2} year^{-1}, respectively, at FK

catchments, and 18.4 mmol m^{-2} year^{-1} and 2.4 mmol m^{-2} year^{-1}, respectively, at MY

catchment. As a result, D_{atm} was estimated to be 69.3 mmol m^{-2} year^{-1} at FK catchments

and 40.1 mmol m^{-2} year^{-1} at MY catchment, using Eq. (3).

3.2 Concentration and isotopic composition of stream nitrate

The concentrations of stream nitrate eluted from the FK1, FK2 (only), and MY

catchments ranged from 97.5 μM to 121.3 μM, from 65.7 μM to 148.5 μM, and from

3.5 μM to 15.3 μM, respectively, with the average concentrations of 109.5 μM, 90.9

μM, and 7.3 μM, respectively, and the standard deviations (SD) of 6.3 μM, 18.5 μM,

and 3.0 μM, respectively, which corresponds to the coefficients of variation (CV) of

5.7 %, 20.4 %, and 40.7 %, respectively (Fig. 2a). All catchments showed no clear

seasonal variation during the observation periods. The variation ranges and the average

concentrations of stream nitrate eluted from the three catchments agreed well with the

past observations performed in the same catchments (Chiwa, 2021).

The stable isotopic compositions of stream nitrate eluted from the FK1, FK2 (only),

and MY catchments ranged from −0.9 ‰ to +1.5 ‰, from −1.4 ‰ to +5.8 ‰, and from

−0.8 ‰ to +2.4 ‰, respectively, for $\delta^{15}N$ (Fig. 2b), from +3.9 ‰ to +8.5 ‰, from −2.2 ‰

to +2.8 ‰, and from −5.6 ‰ to +1.7 ‰, respectively, for $\delta^{18}O$ (Fig. 2c), and from +2.0 ‰

to +3.3 ‰, from +0.6 ‰ to +2.2 ‰, and from +0.2 ‰ to +1.0 ‰, respectively, for $\Delta^{17}O$

(Fig. 2d), with no clear seasonal variation during the observation periods. The

concentration-weighted averages for the $\delta^{15}N$, $\delta^{18}O$, and $\Delta^{17}O$ values of stream nitrate

were +0.2 ‰, +6.4 ‰, and +2.6 ‰, respectively, at FK1, +1.0 ‰, +0.5 ‰, and +1.5 ‰,

respectively, at FK2, +0.7 ‰, −2.5 ‰, and +0.6 ‰, respectively, at MY.

3.3 Concentration of unprocessed atmospheric nitrate and the M_{atm}/D_{atm} ratio in each

catchment

The concentration of unprocessed atmospheric nitrate ($[NO_3^-{}_{atm}]$) in the streams

eluted from the FK1, FK2 (only), and MY catchments ranged from 8.64 to 14.30 μM,

from 2.27 to 10.71 μM, and from 0.03 to 0.46 μM with the average concentration of

10.80 ± 1.30~~65~~, 5.06 ± 0.67~~92~~, and 0.16 ± 0.03~~5~~ μM, respectively, even though these

studied catchments showed little seasonal variations during the observation periods (Fig.

360   2e). The annual export flux of nitrate (M_{total}), the annual export flux of $NO_3^-{}_{atm}$ (M_{atm}),

361   and the M_{atm}/D_{atm} ratio were 98.8 ± 17.8 mmol m^{-2} year^{-1}, $9.7 \pm 2.1\underline{3}$ mmol m^{-2} year^{-1},

362   and $14.1 \pm 4.1\underline{4}$ % at FK1 catchment, respectively, 82.0 ± 14.8 mmol m^{-2} year^{-1}, $4.6 \pm$

363   $1.0\underline{2}$ mmol m^{-2} year^{-1}, and $6.6 \pm 2.0\underline{1}$ % at FK2 catchment, respectively, 23.7 ± 1.2

364   mmol m^{-2} year^{-1}, $0.5 \pm 0.1\underline{2}$ mmol m^{-2} year^{-1}, and $1.3 \pm 0.4\underline{5}$ % at MY catchment,

365   respectively (Table 2). The uncertainties of [$NO_3^-{}_{atm}$], M_{atm}, and M_{atm}/D_{atm} ratio in each

366   catchment were determined from the uncertainties of $\Delta^{17}O$, $\Delta^{17}O_{atm}$, F_{stream}, and D_{atm}

367   according to the equations of error propagation. The details were described in Appendix

368   A.

369

370   **4 Discussion**

371   4.1 Deposition rate of atmospheric nitrate at the study catchments

372   Based on the air monitoring data determined at the stations of Fukuoka (33°51′N,

373   130°50′E) and Miyazaki (31°83′N, 131°42′E) from 2011 to 2017, the Environmental

374   Laboratories Association of Japan (2017) reported D_{atm} to be 57.8 mmol m^{-2} year^{-1} at

375   Fukuoka and 49.1 mmol m^{-2} year^{-1} at Miyazaki. Those values are consistent with the

376   D_{atm} estimated in this study (69.3 and 40.1 mmol m^{-2} year^{-1} at the FK and MY

377   catchments, respectively), within a difference of approximately 20 %. Thus, we

378   concluded that the D_{atm} estimated in this study was reliable within the error margin of

379   20 % (Table 2). Because the D_{atm} determined at the FK catchments was the highest

380   among the forested catchments in Table 3, we further compared the D_{atm} of the FK

381 catchments with those from the other air monitoring stations in Japan reported in past

382 studies, along with that of the MY catchment (Table S1). While the D_{atm} of the MY

383 catchment corresponded to the average level among the sites compiled in Table S1, the

384 D_{atm} of the FK catchments exceeded the average level significantly. In addition, the D_{atm}

385 of the FK catchments corresponded to one of the highest among the Japanese forested

386 areas (Table S1). All the catchments in Japan can be suffered from the long-range

387 transport of air pollutants derived from megacities in East Asian region (Chiwa, 2021;

388 Chiwa et al., 2012 and 2013).In addition, the shorter transport distance from the

389 Fukuoka metropolitan area (total population: 1.62 million people; population density:

390 4715 people/km^2) may be mainly responsible for the D_{atm} higher in FK than in MY,

391 because the FK catchments are only 15 km west of the Fukuoka metropolitan area.

392

393 4.2 Excess leaching of unprocessed atmospheric nitrate from FK catchments

394   The isotopic compositions ($\delta^{15}N$, $\delta^{18}O$, and $\Delta^{17}O$) of stream nitrate eluted from the

395 FK and MY catchments were typical for those eluted from forested catchments (Hattori

396 et al., 2019; Huang et al., 2020; Nakagawa et al., 2013, 2018; Riha et al., 2014; Sabo et

397 al., 2016; Tsunogai et al., 2014, 2016). The striking features found in the FK catchments

398 were that, in addition to the high [NO_3^-] and high M_{total} that had been clarified in a past

399 study (Chiwa, 2021), both [$NO_{3\ atm}^-$] and M_{atm} in FK were higher than those eluted from

400 MY (Table 2). Especially, the average [$NO_{3\ atm}^-$] in the stream eluted from the FK1

401 catchment was the highest ever reported in forested streams determined through

402   continuous monitoring for more than 1 year (Bostic et al., 2021; Bourgeois et al., 2018b,

403   2018a; Hattori et al., 2019; Huang et al., 2020; Nakagawa et al., 2018; Rose et al., 2015;

404   Sabo et al., 2016; Tsunogai et al., 2014, 2016).

405   The observed high $[NO_3^-{}_{atm}]$ in the stream eluted from the FK1 catchment could be

406   caused just by the high $[NO_3^-{}_{atm}]$ ~~in~~ deposition in the catchment. Thus, we compiled all

407   past data ever reported in forested streams through continuous monitoring in Table 3,

408   where the data of average $[NO_3^-]$, average $[NO_3^-{}_{atm}]$, M_{atm}, M_{total}, D_{atm}, and M_{atm}/D_{atm}

409   ratio were included for comparison. The result showed that the M_{atm}/D_{atm} ratio, along

410   with M_{atm}, was the highest as well in the FK1 catchment among the forested catchments

411   (Table 3).

412   Elevated loading of nitrogen through atmospheric deposition was responsible for the

413   occurrence of nitrogen saturation in forest ecosystems, from which elevated levels of

414   nitrate are exported (Aber et al., 1989). Nakagawa et al. (2018) proposed that the

415   M_{atm}/D_{atm} ratio can be an index for evaluating the nitrogen saturation in each forested

416   catchment, because the M_{atm}/D_{atm} ratio directly reflects the present demand for

417   atmospheric nitrate deposited in each forested catchment, and thus reflects the nitrogen

418   saturation in each forested catchment. The high M_{atm}/D_{atm} ratios observed in the FK

419   catchments implied that the demand for atmospheric nitrate was low in the FK

420   catchments and that the stages of nitrogen saturation at the FK catchments were higher

421   than those at other forested catchments. That is, the nitrogen saturation at the FK

422   catchments was responsible for the observed high $[NO_3^-]$ and high M_{total} at the FK

423   catchments than at MY and any other catchment ever studied (Table 3).

424   The stand age of forests can affect the retention or loss of N (Fukushima et al., 2011;

425   Ohrui and Mitchell, 1997). Fukushima et al. (2011) evaluated N uptake rates of

426   Japanese cedars at different ages (5-89 years old) and demonstrated that the N uptake

427   rates of Japanese cedars were higher in younger stands (53 kg N ha^{-1} year^{-1} in 16 years

428   old) than in older stands (29 kg N ha^{-1} year^{-1} in 31 years old; 24 kg N ha^{-1} year^{-1} in 42

429   years old; 34 kg N ha^{-1} year^{-1} in 89 years old). In addition, Yang and Chiwa (2021)

430   found that the nitrate concentration in the soil water taken beneath the rooting zone of

431   matured artificial Japanese cedar plantations (607 $\pm$ 59 µM; 64-69 years old) was

432   significantly higher than that of normal Japanese oak plantations (8.7 $\pm$ 8.1 µM; 24

433   years old). Moreover, by adding ammonium nitrate (50 kg N ha^{-1} year^{-1}) to the forest

434   floor directly, Yang and Chiwa (2021) found that the nitrate concentration in the soil

435   water of the matured artificial Japanese cedar plantations increased significantly faster

436   than that of the normal Japanese oak plantations, probably because of the lower N

437   uptake rates in the matured artificial Japanese cedar plantations. Because most of the

438   artificial Japanese cedar/cypress plantations in the FK and MY catchments have reached

439   their maturity (> 50 years; Yang and Chiwa, 2021), the higher proportion of matured

440   artificial Japanese cedar/cypress plantations in the FK1 catchment (Table 1) was highly

441   responsible for the observed elevated leaching of nitrate, caused by the reduction in N

442   uptake rates.

443   As a result, we concluded that the FK forested catchments were under the high

444   nitrogen saturation stage, FK1 catchment especially, and the nitrogen saturation in the

445   FK1 catchment was responsible for the elevated M_{total}, M_{atm}, $[NO_3^-]$, $[NO_{3\ atm}^-]$ found

446   in the stream eluted from the catchment (Figs. 3a, 3b, 3c, and 3de).

447

448   4.3 The M_{atm}/D_{atm} ratio as an index of nitrogen saturation

449   Past studies have used the concentration of stream nitrate as one of the important

450   indexes to evaluate the stage of nitrogen saturation in each forest (Aber, 1992; Huang

451   et al., 2020; Rose et al., 2015; Stoddard, 1994). The strong linear relationship ($R^2 = 0.76$;

452    $P < 0.0001$) between the stream nitrate concentration and the M_{atm}/D_{atm} ratio, except

453   for the Qingyuan forested catchment (Fig. 3d), further supported that the M_{atm}/D_{atm} ratio

454   can be used as an alternative index of nitrogen saturation, as pointed out in Nakagawa

455   et al. (2018).

456   The differences in the number of storm and/or snowmelt events could affect the

457   M_{atm}/D_{atm} ratio as well, because $NO_{3\ atm}^-$ could be injected into the stream water directly,

458   along with the storm-/-snowmelt water (Tsunogai et al., 2014; Ding et al., 2022; Inamdar

459   and Mitchell, 2006). In recent study, however, we found that the storm events have little

460   impactimpacts on the M_{atm}/D_{atm} ratio, based on monitoring temporal variation of

461    $[NO_{3\ atm}^-]$ in a stream water during storm events (Ding et al., 2022). In addition, the low

462   M_{atm}/D_{atm} ratio found in Uryu forested catchment (0.7 %; Table 3) implied that the

463   snowmelt has little impactimpacts on the M_{atm}/D_{atm} ratio as well, because 30% of the

464   annual mean precipitation was snow in Uryu forested catchment (Tsunogai et al., 2014).

465   The differences in the amount of precipitation, temperature, and the flux of stream

466   water could affect the M_{atm}/D_{atm} ratio as well. As a result, the annual amount of

467   precipitation, mean temperature, and the annual mean flux of stream water (F_{stream}) in

468   the forested catchments were compiled in Table S2. While the stream nitrate

469   concentration showed a~~the~~ strong linear relationship ($R^2 = 0.76$; $P < 0.0001$) with the

470   M_{atm}/D_{atm} ratio (Fig. 3d), the precipitation, temperature, and F_{stream} did not show a

471   significant relationship with the M_{atm}/D_{atm} ratio ($P > 0.14$; Fig. 4). As a result, we

472   concluded that the M_{atm}/D_{atm} ratio was mainly controlled by the progress of nitrogen

473   saturation, rather than the differences in the number of storm and/or snowmelt events,

474   the amount of precipitation, temperature, and the flux of stream water.

475   The differences in the residence time of water in each catchment could also impact

476   the M_{atm}/D_{atm} ratio, as the residence time of water in forested catchments ranges from

477   one month to more than one year (Asano et al., 2002; Farrick and Branfireun, 2015;

478   Kabeya et al., 2008; Rodgers et al., 2005; Soulsby et al., 2006; Tetzlaff et al., 2007). It

479   is difficult to explain high [NO_3^-] and high M_{total} eluted from the catchment by the

480   residence time of water alone, while the M_{atm}/D_{atm} ratio could be higher in catchments

481   with a shorter water residence time, as the majority of nitrate eluted from the catchment

482   with a high M_{atm}/D_{atm} ratio was $NO_{3~re}^-$ produced by microbial nitrification. The

483   significant correlation between M_{total} and M_{atm}/D_{atm} ratios ($P < 0.0001$; Fig. 3a)

484   supported nitrogen saturation as the leading cause of high M_{total} in catchments with a

485   high M_{atm}/D_{atm} ratio. Additionally, the high loading of atmospheric nitrogen, the type of

486   plantation, and the old age of plantation in the FK1 catchment all supported the

487   conclusion that the FK1 catchment was under nitrogen saturation.]

488   The M_{atm}/D_{atm} ratio is a more reliable and robust index than the stream nitrate

489   concentration, as explained below. The Qingyuan forested catchment can be classified

into the highest nitrogen saturation stage based only on the highest stream nitrate

concentration of 150 μM (Table 3). However, based on the leaching flux of nitrogen via

stream water monitored by Huang et al. (2020) for 4 years in the Qingyuan forested

catchment, along with the deposition flux of nitrogen, we can obtain the M_{atm}/D_{atm} ratio

in the catchment to be a medium level of 5.8 ± 1.3 %, implying that the nitrogen

saturation stage was not so high (Table 3). Huang et al. (2020) also concluded that the

input of nitrogen exceeded the output in the catchment, and thus, the catchment was at

stage 2 of nitrogen saturation. The M_{atm}/D_{atm} ratio in the Qingyuan forested catchment

with a medium level among all forested catchments (Fig. 3d) should be a more reliable

index of nitrogen saturation.

Compared with those in the other forested catchments in Table 3, the annual amount

of precipitation (P) has the lowest value of 709 mm in the Qingyuan forested catchment.

The flux of stream water (F_{stream}) has the lowest value of 309 mm as well. Thus, we

concluded that nitrate was relatively concentrated in the catchment because of the small

precipitation, resulting in relative enrichment in the concentrations of both nitrate (150

μM) and unprocessed atmospheric nitrate (8.9 μM) in the stream.

While the concentration of stream nitrate, as an index of nitrogen saturation

traditionally, can be influenced by the amount of precipitation, as demonstrated in the

Qingyuan forested catchment, the M_{atm}/D_{atm} ratio is independent of the amount of

precipitation (Fig. 4). Therefore, the M_{atm}/D_{atm} ratio can be used as a more robust index

for evaluating nitrogen saturation in each forested catchment.

511 ~~The only concern on using the M_{atm}/D_{atm} ratio as the index of nitrogen saturation is~~

512 ~~the impact of the differences in the residence time of water in each catchment. The~~

513 ~~residence time of water varies from 1 month to more than 1 year in forested catchments~~

514 ~~(Asano et al., 2002; Farrick and Branfireun, 2015; Kabeya et al., 2008; Rodgers et al.,~~

515 ~~2005; Soulsby et al., 2006; Tetzlaff et al., 2007). The M_{atm}/D_{atm} ratio could be lower in~~

516 ~~catchments with longer residence time of water.~~

517 ~~We would like to clarify this in future studies by adding much more data of stream~~

518 ~~nitrate eluted from various forested catchments.~~

519

5 Conclusions

521 Both the concentrations and $\Delta^{17}O$ of stream nitrate were determined for more than 2

522 years in the forested catchments of FK (FK1 and FK2) and MY to determine the

523 M_{atm}/D_{atm} ratio for each catchment. The FK catchments exhibited higher M_{atm}/D_{atm} ratio

524 than the MY catchment and other forested catchments reported in past studies, implying

525 that the progress of nitrogen saturation in the FK catchments was severe. Both age and

526 proportion of artificial plantation in the FK catchments were responsible for the

527 progress of nitrogen saturation. In addition, although past studies have commonly used

528 the concentration of stream nitrate as an index to evaluate the progress of nitrogen

529 saturation in forested catchments, it can be influenced by the amount of precipitation.

530 As a result, we concluded that the M_{atm}/D_{atm} ratio should be used as a more reliable

531 index for evaluating the progress of nitrogen saturation because the M_{atm}/D_{atm} ratio is

532 independent from the amount of precipitation.

533

534 Appendix A: Calculating of uncertainties in the values of $[NO_3^-{}_{atm}]$, M_{atm}, and M_{atm}/D_{atm}

535 ratio

536 The uncertainty in the values of $[NO_3^-{}_{atm}]$ was estimated from the uncertainties in

537 the $\Delta^{17}O$ values of stream nitrate ($\Delta^{17}O$) and $NO_3^-{}_{atm}$ ($\Delta^{17}O_{atm}$) according to the

538 divisive equation of error propagation (A1):

539 $$\sigma_{[NO_3^-{}_{atm}]} = [NO_3^-] * \sqrt{\left(\frac{1}{\Delta^{17}O_{atm}} * \sigma_{\Delta^{17}O}\right)^2 + \left(\frac{\Delta^{17}O}{\Delta^{17}O_{atm}^2} * \sigma_{\Delta^{17}O_{atm}}\right)^2} \qquad (A1)$$

540 where $\sigma_{[NO_3^-{}_{atm}]}$, $\sigma_{\Delta^{17}O}$, and $\sigma_{\Delta^{17}O_{atm}}$ denote the uncertainties in $[NO_3^-{}_{atm}]$, $\Delta^{17}O$ values

541 of stream nitrate, and $\Delta^{17}O$ values of $NO_3^-{}_{atm}$, respectively. The standard error of the

542 mean (SE) of ± 0.1 ‰ and the areal/seasonal variations of ± 3 ‰ was used in

543 calculating $\sigma_{\Delta^{17}O}$ and $\sigma_{\Delta^{17}O_{atm}}$, respectively. As a result, the uncertainty in $[NO_3^-{}_{atm}]$

544 ($\sigma_{[NO_3^-{}_{atm}]}$) was ± 1.30, ± 0.67, and ± 0.03 µM at FK1, FK2, and MY catchments,

545 respectively.

546 The uncertainty in the values of M_{atm} was estimated from the uncertainties in

547 $[NO_3^-{}_{atm}]$ and in F_{stream} according to the multiplicative equation of error propagation

548 (A2):

549 $$\sigma_{M_{atm}} = \sqrt{\left(F_{stream} * \sigma_{[NO_3^-{}_{atm}]}\right)^2 + \left([NO_3^-{}_{atm}] * \sigma_{F_{stream}}\right)^2} \qquad (A2)$$

550 where $\sigma_{M_{atm}}$, $\sigma_{[NO_3^-{}_{atm}]}$, and $\sigma_{F_{stream}}$ denote the uncertainties in M_{atm}, $[NO_3^-{}_{atm}]$, and

551 F_{stream}, respectively. Komatsu et al. (2008) proposed the uncertainty in F_{stream} to be

552 ± 162.3 mm when using the water balance method in estimating F_{stream}. Here, the

553 uncertainty in M_{atm} ($\sigma_{M_{atm}}$) was ± 2.1, ± 1.0, and ± 0.1 mmol m^{-2} yr^{-1} at FK1, FK2, and

554 MY catchments, respectively.

555 The uncertainty in M_{atm}/D_{atm} ratio was estimated from the uncertainties in M_{atm} and

in D_{atm} according to the divisive equation of error propagation (A3):

$$\sigma_{M_{atm}/D_{atm}\ ratio} = \sqrt{\left(\frac{1}{D_{atm}} * \sigma_{M_{atm}}\right)^2 + \left(\frac{M_{atm}}{D_{atm}^2} * \sigma_{D_{atm}}\right)^2} \tag{A3}$$

where $\sigma_{M_{atm}/D_{atm}\ ratio}$, $\sigma_{M_{atm}}$, and $\sigma_{D_{atm}}$ denote the uncertainty in M_{atm}/D_{atm} ratio, M_{atm}, and D_{atm}, respectively. Comparing the deposition rate of $NO_3^-{}_{atm}$ obtained at the other atmospheric monitoring stations nearby, the uncertainty of 20 % was adopted for those of D_{atm} in each catchment, which corresponds to the uncertainty in D_{atm} of $\pm13.9, \pm13.9, \pm8.0$ mmol m^{-2} yr^{-1} at FK1, FK2, and MY catchments, respectively. As a result, the uncertainty in M_{atm}/D_{atm} ratio was ±4.1 %, ±2.0 %, and ±0.4 % at FK1, FK2, and MY catchments, respectively.

Data availability. All the primary data are presented in the Supplement. The other data are available upon request to the corresponding author (Weitian Ding).

Author contributions. UT, FN, KS, and MC designed the study. MC and TK performed the field observations. WD, UT, and FN determined the concentrations and isotopic compositions of the samples. WD, TS, FN, and UT performed data analysis, and WD and UT wrote the paper with input from MC, TK, and KS.

Competing interests. The authors declare that they have no conflict of interest.

Acknowledgements.

577   We thank anonymous referees for valuable remarks on an earlier version of this paper.

578   We also thank Daisuke Nanki, Takuma Nakamura, and Yuko Muramatsu for their

579   long-term water sampling. Additionally, we are grateful to the members of the

580   Biogeochemistry Group, Graduate School of Environmental Studies, Nagoya

581   University, for their valuable support throughout this study. This work was supported

582   by a Grant-in-Aid for Scientific Research from the Ministry of Education, Culture,

583   Sports, Science, and Technology of Japan under grant numbers 22H00561, and

584   17H00780, the Yanmar Environmental Sustainability Support Association, and the

585   River fund of the river foundation, Japan. Weitian Ding would like to take this

586   opportunity to thank the "Nagoya University Interdisciplinary Frontier Fellowship"

587   supported by Nagoya University and JST, the establishment of university fellowships

588   towards the creation of science technology innovation, Grant Number JPMJFS2120.

589

Reference

591   Aber, J. D.: Nitrogen cycling and nitrogen saturation in temperate forest ecosystems,

592   Trends Ecol. Evol., 7(7), 220–224, doi:10.1016/0169-5347(92)90048-G, 1992.

593   Aber, J. D., Nadelhoffer, K. J., Steudler, P. and Melillo, J. M.: Nitrogen Saturation in

594   Northern Forest Ecosystems, Bioscience, 39(6), 378–386, doi:10.2307/1311067,

595   1989.

596   Aikawa, M., Hiraki, T., Tamaki, M. and Shoga, M.: Difference between filtering-type

597   bulk and wet-only data sets based on site classification, Atmos. Environ., 37(19),

598   2597–2603, doi:10.1016/S1352-2310(03)00214-0, 2003.

599   Alexander, B., Hastings, M. G., Allman, D. J., Dachs, J., Thornton, J. A. and

600   Kunasek, S. A.: Quantifying atmospheric nitrate formation pathways based on a

601   global model of the oxygen isotopic composition ($\delta^{17}O$) of atmospheric nitrate,

602   Atmos. Chem. Phys., 9(14), 5043–5056, doi:10.5194/acp-9-5043-2009, 2009.

603   Asano, Y., Uchida, T. and Ohte, N.: Residence times and flow paths of water in steep

604   unchannelled catchments, Tanakami, Japan, J. Hydrol., 261(1–4), 173–192,

605   doi:10.1016/S0022-1694(02)00005-7, 2002.

606   Environmental Laboratories Association of Japan: Acid Rain National Survey Report

607   2017, https://tenbou.nies.go.jp/envgis_explain/acid_rain/content.html.

608   Bostic, J. T., Nelson, D. M., Sabo, R. D. and Eshleman, K. N.: Terrestrial Nitrogen

609   Inputs Affect the Export of Unprocessed Atmospheric Nitrate to Surface Waters:

610   Insights from Triple Oxygen Isotopes of Nitrate, Ecosystems, doi:10.1007/s10021-

611   021-00722-9, 2021.

612   Bourgeois, I., Savarino, J., Némery, J., Caillon, N., Albertin, S., Delbart, F., Voisin,

613   D. and Clément, J. C.: Atmospheric nitrate export in streams along a montane to

614   urban gradient, Sci. Total Environ., 633, 329–340,

615   doi:10.1016/j.scitotenv.2018.03.141, 2018a.

616   Bourgeois, I., Savarino, J., Caillon, N., Angot, H., Barbero, A., Delbart, F., Voisin, D.

617   and Clément, J. C.: Tracing the Fate of Atmospheric Nitrate in a Subalpine Watershed

618   Using $\Delta^{17}O$, Environ. Sci. Technol., 52(10), 5561–5570, doi:10.1021/acs.est.7b02395,

619   2018b.Chiwa, M.: Ten-year determination of atmospheric phosphorus deposition at

620   three forested sites in Japan, Atmos. Environ., 223(May 2019), 1–7,

621   doi:10.1016/j.atmosenv.2019.117247, 2020.

622   Chiwa, M.: Long-term changes in atmospheric nitrogen deposition and stream water

623   nitrate leaching from forested watersheds in western Japan, Environ. Pollut.,

624   287(November 2020), 117634, doi:10.1016/j.envpol.2021.117634, 2021.

625   Chiwa, M., Enoki, T., Higashi, N., Kumagai, T. and Otsuki, K.: The Increased

626   Contribution of Atmospheric Nitrogen Deposition to Nitrogen Cycling in a Rural

627   Forested Area of Kyushu, Japan, Water, Air, Soil Pollut., 224(11), 1763,

628   doi:10.1007/s11270-013-1763-2, 2013.

629   Chiwa, M., Onikura, N., Ide, J. and Kume, A.: Impact of N-Saturated Upland Forests

630   on Downstream N Pollution in the Tatara River Basin, Japan, Ecosystems, 15(2),

631   230–241, doi:10.1007/s10021-011-9505-z, 2012.

632   Chiwa, M.: Characteristics of atmospheric nitrogen and sulfur containing compounds

633   in an inland suburban-forested site in northern Kyushu, western Japan, Atmos. Res.,

634   96(4), 531–543, doi:10.1016/j.atmosres.2010.01.001, 2010.

635   Ding, W., Tsunogai, U., Nakagawa, F., Sambuichi, T., Sase, H., Morohashi, M., and

636   Yotsuyanagi, H.: Tracing the source of nitrate in a forested stream showing elevated

637   concentrations during storm events, Biogeosciences, 19, 3247–3261,

638   https://doi.org/10.5194/bg-19-3247-2022, 2022.

639 Endo, T., Yagoh, H., Sato, K., Matsuda, K., Hayashi, K., Noguchi, I. and Sawada, K.:

640 Regional characteristics of dry deposition of sulfur and nitrogen compounds at

641 EANET sites in Japan from 2003 to 2008, Atmos. Environ., 45(6), 1259–1267,

642 doi:10.1016/j.atmosenv.2010.12.003, 2011.

643 Farrick, K. K. and Branfireun, B. A.: Flowpaths, source water contributions and water

644 residence times in a Mexican tropical dry forest catchment, J. Hydrol., 529, 854–865,

645 doi:10.1016/j.jhydrol.2015.08.059, 2015.Kabeya, N., Shimizu, A., Nobuhiro, T. and

646 Tamai, K.: Preliminary study of flow regimes and stream water residence times in

647 multi-scale forested watersheds of central Cambodia, Paddy Water Environ., 6(1), 25–

648 35, doi:10.1007/s10333-008-0104-3, 2008.

649 Fukushima, K., Tateno, R. and Tokuchi, N.: Soil nitrogen dynamics during stand

650 development after clear-cutting of Japanese cedar (Cryptomeria japonica) plantations,

651 J. For. Res., 16(5), 394–404, doi:10.1007/s10310-011-0286-1, 2011.

652 Galloway, J. N., Aber, J. D., Erisman, J. W., Seitzinger, S. P., Howarth, R. W.,

653 Cowling, E. B. and Cosby, B. J.: The nitrogen cascade, Bioscience, 53(4), 341–356,

654 doi:10.1641/0006-3568(2003)053[0341:TNC]2.0.CO;2, 2003.

655 Hattori, S., Nuñez Palma, Y., Itoh, Y., Kawasaki, M., Fujihara, Y., Takase, K. and

656 Yoshida, N.: Isotopic evidence for seasonality of microbial internal nitrogen cycles in

657 a temperate forested catchment with heavy snowfall, Sci. Total Environ., 690, 290–

658 299, doi:10.1016/j.scitotenv.2019.06.507, 2019.

659 Hirota, A., Tsunogai, U., Komatsu, D. D. and Nakagawa, F.: Simultaneous

660   determination of $\delta^{15}N$ and $\delta^{18}O$ of N_2O and $\delta^{13}C$ of CH_4 in nanomolar quantities from

661   a single water sample, Rapid Commun. Mass Spectrom., 24, 1085–1092,

662   doi:10.1002/rcm.4483, 2010.

663   Huang, S., Wang, F., Elliott, E. M., Zhu, F., Zhu, W., Koba, K., Yu, Z., Hobbie, E.

664   A., Michalski, G., Kang, R., Wang, A., Zhu, J., Fu, S. and Fang, Y.: Multiyear

665   Measurements on $\Delta^{17}O$ of Stream Nitrate Indicate High Nitrate Production in a

666   Temperate Forest, Environ. Sci. Technol., 54(7), 4231–4239,

667   doi:10.1021/acs.est.9b07839, 2020.

668   Inoue, T., Nakagawa, F., Shibata, H. and Tsunogai, U.: Vertical Changes in the Flux

669   of Atmospheric Nitrate From a Forest Canopy to the Surface Soil Based on $\Delta^{17}O$

670   Values, J. Geophys. Res. Biogeosciences, 126(4), 1–18, doi:10.1029/2020JG005876,

671   2021.

672   Inamdar, S. P. and Mitchell, M. J.: Hydrologic and topographic controls on storm-

673   event exports of dissolved organic carbon (BOC) and nitrate across catchment scales,

674   Water Resour. Res., 42(3), 1–16, doi:10.1029/2005WR004212, 2006.

675   Kaiser, J., Hastings, M. G., Houlton, B. Z., Röckmann, T. and Sigman, D. M.: Triple

676   oxygen isotope analysis of nitrate using the denitrifier method and thermal

677   decomposition of N_2O, Anal. Chem., 79(2), 599–607, doi:10.1021/ac061022s, 2007.

678   Komatsu, D. D., Ishimura, T., Nakagawa, F. and Tsunogai, U.: Determination of the

679    $^{15}N/^{14}N$, $^{17}O/^{16}O$, and $^{18}O/^{16}O$ ratios of nitrous oxide by using continuous-flow

680   isotope-ratio mass spectrometry Daisuke, Rapid Commun. Mass Spectrom., 22, 1587–

681   1596, doi:10.1002/rcm.3493, 2008a.

682   Komatsu, H., Maita, E. and Otsuki, K.: A model to estimate annual forest

683   evapotranspiration in Japan from mean annual temperature, , 330–340,

684   doi:10.1016/j.jhydrol.2007.10.006, 2008b.

685   Konno, U., Tsunogai, U., Komatsu, D. D., Daita, S., Nakagawa, F., Tsuda, A.,

686   Matsui, T., Eum, Y. J. and Suzuki, K.: Determination of total N_2 fixation rates in the

687   ocean taking into account both the particulate and filtrate fractions, Biogeosciences,

688   7(8), 2369–2377, doi:10.5194/bg-7-2369-2010, 2010.

689   Matsuda, K.: Estimation of dry deposition for sulfur and nitrogen compounds in the

690   atmosphere : Updated parameterization of deposition velocity, J. Japan Soc. Atmos.

691   Environ., 43(6), 332–339, doi:10.11298/taiki1995.43.332, 2008.

692   McIlvin, M. R. and Altabet, M. A.: Chemical conversion of nitrate and nitrite to

693   nitrous oxide for nitrogen and oxygen isotopic analysis in freshwater and seawater,

694   Anal. Chem., 77(17), 5589–5595, doi:10.1021/ac050528s, 2005.

695   Michalski, G., Scott, Z., Kabiling, M. and Thiemens, M. H.: First measurements and

696   modeling of $\Delta^{17}O$ in atmospheric nitrate, Geophys. Res. Lett., 30(16), 3–6,

697   doi:10.1029/2003GL017015, 2003.

698   Michalski, G., Meixner, T., Fenn, M., Hernandez, L., Sirulnik, A., Allen, E. and

699   Thiemens, M.: Tracing Atmospheric Nitrate Deposition in a Complex Semiarid

700   Ecosystem Using $\Delta^{17}O$, Environ. Sci. Technol., 38(7), 2175–2181,

701   doi:10.1021/es034980+, 2004.

702 Mitchell, M. J., Iwatsubo, G., Ohrui, K. and Nakagawa, Y.: Nitrogen saturation in

703 Japanese forests: An evaluation, For. Ecol. Manage., 97(1), 39–51,

704 doi:10.1016/S0378-1127(97)00047-9, 1997.

705 Morin, S., Sander, R. and Savarino, J.: Simulation of the diurnal variations of the

706 oxygen isotope anomaly ($\Delta^{17}O$) of reactive atmospheric species, Atmos. Chem. Phys.,

707 11(8), 3653–3671, doi:10.5194/acp-11-3653-2011, 2011.

708 Nakagawa, F., Suzuki, A., Daita, S., Ohyama, T., Komatsu, D. D. and Tsunogai, U.:

709 Tracing atmospheric nitrate in groundwater using triple oxygen isotopes: Evaluation

710 based on bottled drinking water, Biogeosciences, 10(6), 3547–3558, doi:10.5194/bg-

711 10-3547-2013, 2013.

712 Nakagawa, F., Tsunogai, U., Obata, Y., Ando, K., Yamashita, N., Saito, T.,

713 Uchiyama, S., Morohashi, M. and Sase, H.: Export flux of unprocessed atmospheric

714 nitrate from temperate forested catchments: A possible new index for nitrogen

715 saturation, Biogeosciences, 15(22), 7025–7042, doi:10.5194/bg-15-7025-2018, 2018.

716 Nelson, D. M., Tsunogai, U., Ding, D., Ohyama, T., Komatsu, D. D., Nakagawa, F.,

717 Noguchi, I. and Yamaguchi, T.: Triple oxygen isotopes indicate urbanization affects

718 sources of nitrate in wet and dry atmospheric deposition, Atmos. Chem. Phys., 18(9),

719 6381–6392, doi:10.5194/acp-18-6381-2018, 2018.

720 Ohrui, K. and Mitchell, M. J.: Nitrogen Saturation in Japanese Forested Watersheds

721 Author (s): Kiyokazu Ohrui and Myron J . Mitchell Published by : Wiley Stable

722 URL : http://www.jstor.org/stable/2269507 Accessed : 05-07-2016 04 : 51 UTC Your

723   use of the JSTOR archive indicates your ac, , 7(2), 391–401, 1997.

724   Paerl, H. W. and Huisman, J.: Climate change: A catalyst for global expansion of

725   harmful cyanobacterial blooms, Environ. Microbiol. Rep., 1(1), 27–37,

726   doi:10.1111/j.1758-2229.2008.00004.x, 2009.

727   Peterjohn, W. T., Adams, M. B. and Gilliam, F. S.: Symptoms of nitrogen saturation

728   in two central Appalachian hardwood forest ecosystems, Biogeochemistry, 35(3),

729   507–522, doi:10.1007/BF02183038, 1996.

730   Riha, K. M., Michalski, G., Gallo, E. L., Lohse, K. A., Brooks, P. D. and Meixner, T.:

731   High Atmospheric Nitrate Inputs and Nitrogen Turnover in Semi-arid Urban

732   Catchments, Ecosystems, 17(8), 1309–1325, doi:10.1007/s10021-014-9797-x, 2014.

733   Rodgers, P., Soulsby, C., Waldron, S. and Tetzlaff, D.: Using stable isotope tracers to

734   identify hydrological flow paths, residence times and landscape controls in a

735   mesoscale catchment, Hydrol. Earth Syst. Sci. Discuss., 9, 139–155, 2005.Rose, L.

736   A., Elliott, E. M. and Adams, M. B.: Triple Nitrate Isotopes Indicate Differing Nitrate

737   Source Contributions to Streams Across a Nitrogen Saturation Gradient, Ecosystems,

738   18(7), 1209–1223, doi:10.1007/s10021-015-9891-8, 2015.

739   Sabo, R. D., Nelson, D. M. and Eshleman, K. N.: Episodic, seasonal, and annual

740   export of atmospheric and microbial nitrate from a temperate forest, Geophys. Res.

741   Lett., 43(2), 683–691, doi:10.1002/2015GL066758, 2016.

742   Sappa, G., Ferranti, F. and Pecchia, G. M.: Validation Of Salt Dilution Method For

743   Discharge Measurements In The Upper Valley Of Aniene River (Central Italy), Recent

744   Adv. Environ. Ecosyst. Dev., (October 2015), 42–48, 2015.

745   Soulsby, C., Tetzlaff, D., Rodgers, P., Dunn, S. and Waldron, S.: Runoff processes,

746   stream water residence times and controlling landscape characteristics in a mesoscale

747   catchment: An initial evaluation, J. Hydrol., 325(1–4), 197–221,

748   doi:10.1016/j.jhydrol.2005.10.024, 2006.

749   Stoddard, J. L.: Long-Term Changes in Watershed Retention of Nitrogen, , 223–284,

750   doi:10.1021/ba-1994-0237.ch008, 1994.

751   Tetzlaff, D., Malcolm, I. A. and Soulsby, C.: Influence of forestry, environmental

752   change and climatic variability on the hydrology, hydrochemistry and residence times

753   of upland catchments, J. Hydrol., 346(3–4), 93–111,

754   doi:10.1016/j.jhydrol.2007.08.016, 2007.

755   Tsunogai, U., Komatsu, D. D., Daita, S., Kazemi, G. A., Nakagawa, F., Noguchi, I.

756   and Zhang, J.: Tracing the fate of atmospheric nitrate deposited onto a forest

757   ecosystem in Eastern Asia using $\Delta^{17}O$, Atmos. Chem. Phys., 10(4), 1809–1820,

758   doi:10.5194/acp-10-1809-2010, 2010.

759   Tsunogai, U., Daita, S., Komatsu, D. D., Nakagawa, F. and Tanaka, A.: Quantifying

760   nitrate dynamics in an oligotrophic lake using $\Delta^{17}O$, Biogeosciences, 8(3), 687–702,

761   doi:10.5194/bg-8-687-2011, 2011.

762   Tsunogai, U., Komatsu, D. D., Ohyama, T., Suzuki, A., Nakagawa, F., Noguchi, I.,

763   Takagi, K. and Nomura, M.: Quantifying the effects of clear-cutting and strip-cutting

764   on nitrate dynamics in a forested watershed using triple oxygen isotopes as tracers, ,

765   (1), 5411–5424, doi:10.5194/bg-11-5411-2014, 2014.

766   Tsunogai, U., Miyauchi, T., Ohyama, T., Komatsu, D. D., Nakagawa, F., Obata, Y.,

767   Sato, K. and Ohizumi, T.: Accurate and precise quantification of atmospheric nitrate

768   in streams draining land of various uses by using triple oxygen isotopes as tracers,

769   Biogeosciences, 13(11), 3441–3459, doi:10.5194/bg-13-3441-2016, 2016.

770   Tsunogai, U., Miyauchi, T., Ohyama, T., Komatsu, D. D., Ito, M. and Nakagawa, F.:

771   Quantifying nitrate dynamics in a mesotrophic lake using triple oxygen isotopes as

772   tracers, Limnol. Oceanogr., 63, S458–S476, doi:10.1002/lno.10775, 2018.

773   Vitousek, P. M. and Howarth, R. W.: Nitrogen limitation on land and in the sea: How

774   can it occur?, Biogeochemistry, 13(2), 87–115, doi:10.1007/BF00002772, 1991.

775   Watanabe, M., Miura, S., Hasegawa, S., Koshikawa, M. K., Takamatsu, T., Kohzu,

776   A., Imai, A. and Hayashi, S.: Coniferous coverage as well as catchment steepness

777   influences local stream nitrate concentrations within a nitrogen-saturated forest in

778   central Japan, Sci. Total Environ., 636, 539–546, doi:10.1016/j.scitotenv.2018.04.307,

779   2018.

780   Yamazaki, A., Watanabe, T. and Tsunogai, U.: Nitrogen isotopes of organic nitrogen

781   in reef coral skeletons as a proxy of tropical nutrient dynamics, Geophys. Res. Lett.,

782   38(19), 1–5, doi:10.1029/2011GL049053, 2011.

783   Yang, R. and Chiwa, M.: Low nitrogen retention in a Japanese cedar plantation in a

784   suburban area, western Japan, Sci. Rep., 11(1), 1–7, doi:10.1038/s41598-021-84753-

785   1, 2021.

 Table 1. Plant information for each forested catchment (Chiwa, 2021).

Overstory vegetation (%)	FK1	FK2	MY
Artificial Japanese cedar/cypress plantation	74	40	16
Other artificial coniferous plantations	<1	<1	7
Natural trees	10	54	75
Others	16	5	2

787

788

789

Table 2. Average concentrations of stream nitrate ($[NO_3^-]_{avg}$), the average concentrations of unprocessed $NO_3^-{}_{atm}$ in streams ($[NO_3^-{}_{atm}]_{avg}$), the annual export flux of NO_3^- per unit area of catchments (M_{total}), the annual export flux of $NO_3^-{}_{atm}$ per unit area of catchments (M_{atm}), the deposition flux of $NO_3^-{}_{atm}$ per unit area of catchment (D_{atm}), and the M_{atm}/D_{atm} ratios in the study catchments.

	FK1	FK2	MY
$[NO_3^-]_{avg}$ (μM)	109.5	90.9	7.3
$[NO_3^-{}_{atm}]_{avg}$ (μM)	10.80 ± 1.30~~65~~	5.06 ± 0.67~~92~~	0.16 ± 0.03~~5~~
M_{total} (mmol m^{-2} yr^{-1})	98.8 ± 17.8	82.0 ± 14.8	23.7 ± 1.2
M_{atm} (mmol m^{-2} yr^{-1})	9.7 ± 2.1~~3~~	4.6 ± 1.0~~2~~	0.5 ± 0.1~~2~~
D_{atm} (mmol m^{-2} yr^{-1})	69.3 ± 13.9	69.3 ± 13.9	40.1 ± 8.0
M_{atm}/D_{atm} (%)	14.1 ± 4.1~~4~~	6.6 ± 2.0~~1~~	1.3 ± 0.4~~5~~

795

Table 3. The annual amount of precipitation (P), the average concentration of stream nitrate ($[NO_3^-]_{avg}$), the nitrogen saturation stage, the average concentration of unprocessed $NO_3^-{}_{atm}$ in streams ($[NO_3^-{}_{atm}]_{avg}$), the annual export flux of NO_3^- per unit area of catchment (M_{total}), the annual export flux of $NO_3^-{}_{atm}$ per unit area of catchment (M_{atm}), the deposition flux of $NO_3^-{}_{atm}$ per unit area of catchment (D_{atm}), and the M_{atm}/D_{atm} ratio in the FK1, FK2, and MY, along with those in the catchments studied in past studies using $\Delta^{17}O$ of nitrate as a tracer.

	P	$[NO_3^-]_{avg}$	N stage[*]	$[NO_3^-{}_{atm}]_{avg}$	M_{atm}	M_{total}	D_{atm}	M_{atm}/D_{atm}
	mm	μM		μM	\multicolumn{3}{c}{mmol m^{-2} yr^{-1}}		%
FK1[a]	1777	109.5	-	10.8	9.7	98.8	69.3	14.1
FK2[a]	1777	90.9	-	5.06	4.6	82.0	69.3	6.6
MY[a]	3981	7.3	-	0.2	0.5	23.7	40.1	1.3
KJ[b]	2500	58.4	-	3.3	4.3	76.4	45.6	9.4
IJ1[b]	3300	24.4	2	1.4	2.9	50.1	44.5	6.5
IJ2[b]	3300	17.1	-	0.6	1.2	35.1	44.5	2.6
Fernow1[c]	1450	17.9	1	1.6	0.8	9.3	23.4	3.6
Fernow2[c]	1450	34.3	2	3.4	1.5	14.8	23.4	6.3
Fernow3[c]	1450	60.0	3	4.2	2.4	34.5	23.4	10.3
Uryu[d]	1170	0.7	-	0.1	0.1	1.0	18.6	0.7
Qingyuan[e]	709	150.0	2	8.9	2.9	49.3	50.0	5.8

a: This study

b: Nakagawa et al., 2018; Nakahara et al., 2010

c: Rose et al., 2015

d: Tsunogai et al., 2014

e: Huang et al., 2020

*: N saturation stage estimated in past studies

-: No data
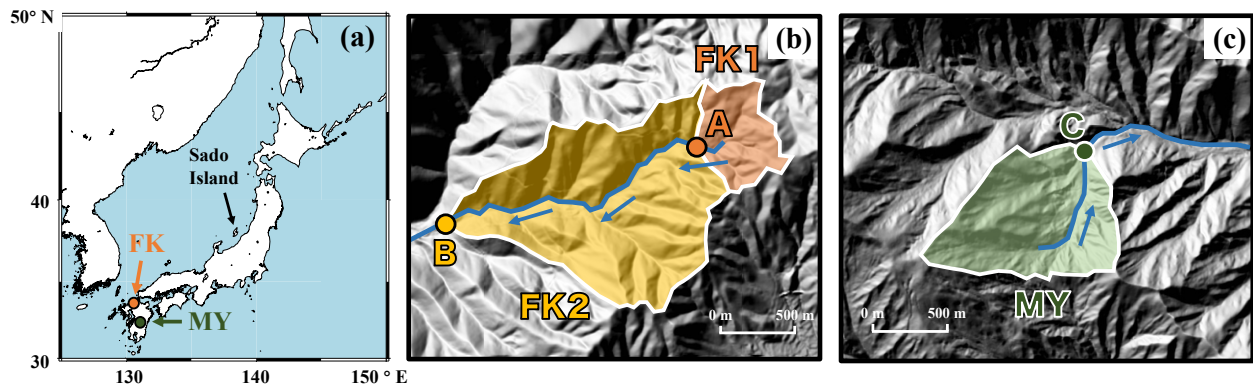
810 **Figure 1.** A map showing the locations of the study catchments (FK and MY) in Japan

811 (a), and the maps of FK1, FK2 (b) and MY catchments (c), shown by orange, yellow,

812 and green areas, respectively, together with the sampling station A, B, and C,

813 respectively, shown by orange, yellow, and green circles, respectively. The blue arrows

814 indicate the flow direction of stream water.

815

816

817

818

819

820

821

822

823

824

825
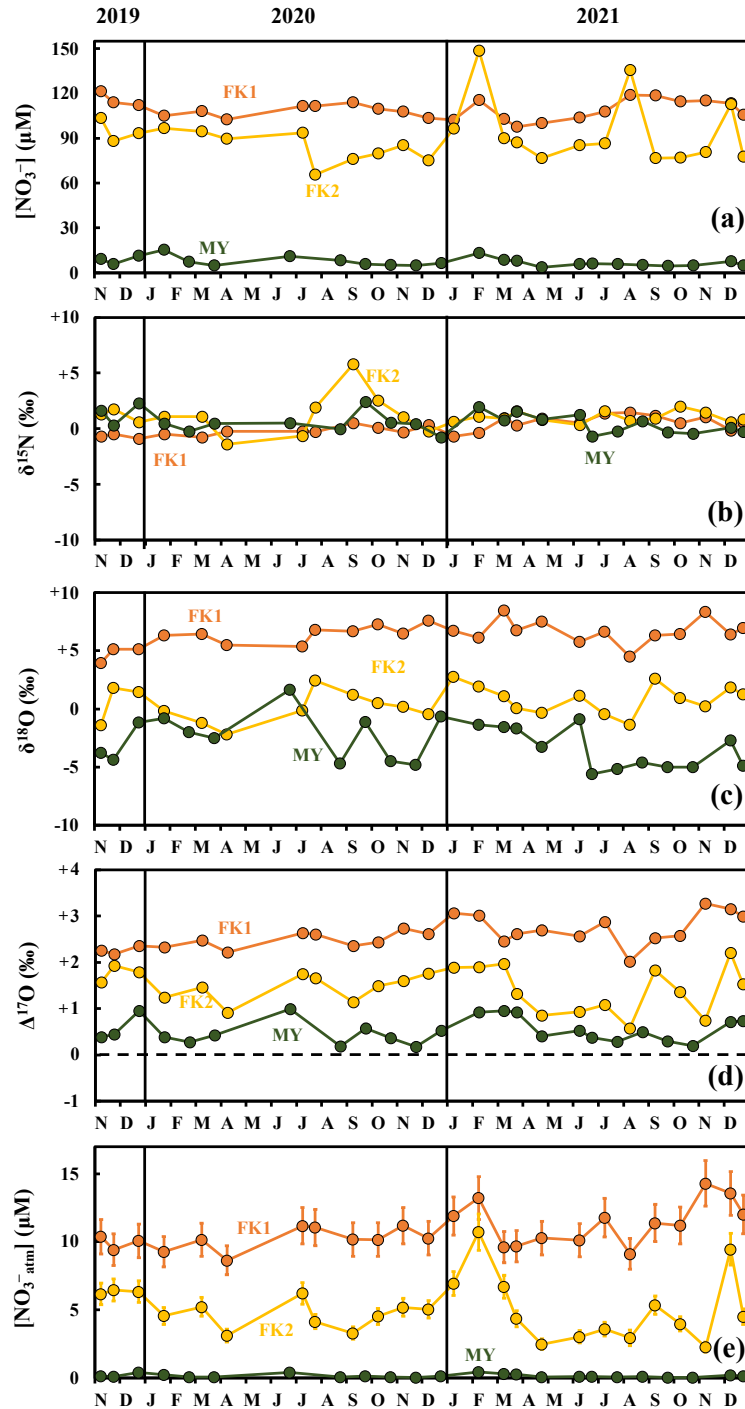
Figure 2. Temporal variations in concentrations of stream nitrate (FK1: orange circles;

FK2: yellow circles; MY: green circles) (a), together with those in $\delta^{15}N$ (b), $\delta^{18}O$ (c),

and $\Delta^{17}O$ (d) of nitrate, and the concentration of unprocessed $NO_3^-{}_{atm}$ ([$NO_3^-{}_{atm}$]) (e) in

the stream water of the FK1, FK2, and MY forested catchments. Error bars smaller than

the sizes of the symbols are not presented.

FK1 ⬤ FK2 ⬤ MY ⬤ ☐ KJ, IJ1, and IJ2 (Nakagawa et al., 2018)

△ Uryu (Tsunogai et al., 2014) ◇ Fernow 1, 2, and 3 (Rose et al., 2015)

◯ Qingyuan (Huang et al., 2020)
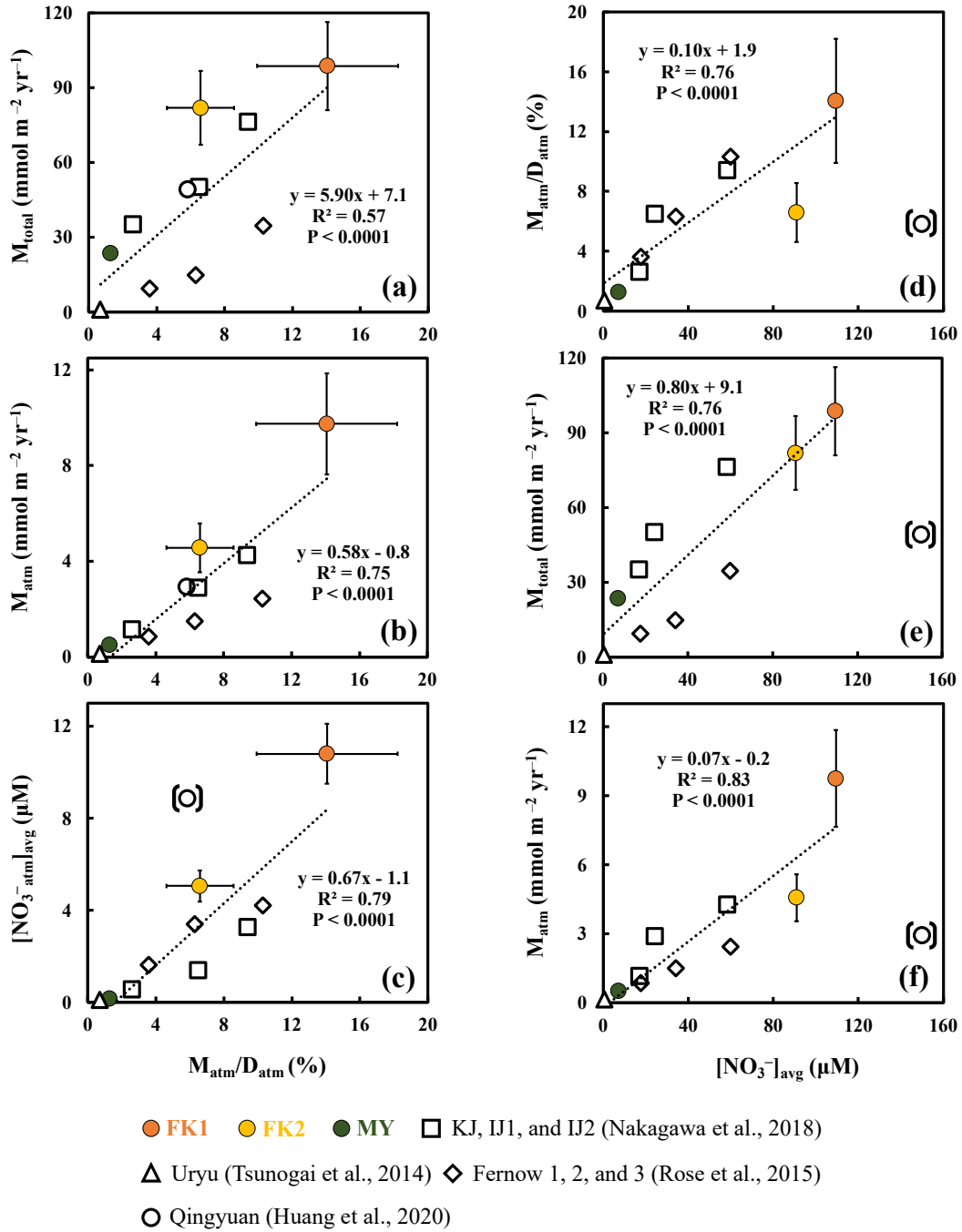
Figure 3. Annual export flux of nitrate per unit area (M_{total}) plotted as a function of the

M_{atm}/D_{atm} ratio in each forested catchment (a); the annual export flux of unprocessed

atmospheric nitrate per unit area (M_{atm}) plotted as a function of the M_{atm}/D_{atm} ratio (b);

the average concentration of $NO_3^-{}_{atm}$ ([$NO_3^-{}_{atm}$]$_{avg}$) plotted as a function of the

M_{atm}/D_{atm} ratio (c); the M_{atm}/D_{atm} ratio plotted as a function of the average concentration

of nitrate ($[NO_3^-]_{avg}$) (d); the M_{total} plotted as a function of $[NO_3^-]_{avg}$ (e); the M_{atm}

plotted as a function of $[NO_3^-]_{avg}$ (f) (FK1: orange circles; FK2: yellow circles; MY:

green circles). Those determined for the forested catchments in past studies are plotted

as well (Qingyuan: white circle (Huang et al., 2020); KJ, IJ1, and IJ2: white squares

(Nakagawa et al., 2018); Fernow 1, 2, and 3: white diamonds (Lucy et al., 2015); Uryu:

white triangle (Tsunogai., 2014)). The data obtained in the Qingyuan forested

catchment are shown in parentheses and excluded from the calculation to estimate

correlation coefficients (see text for the reason).
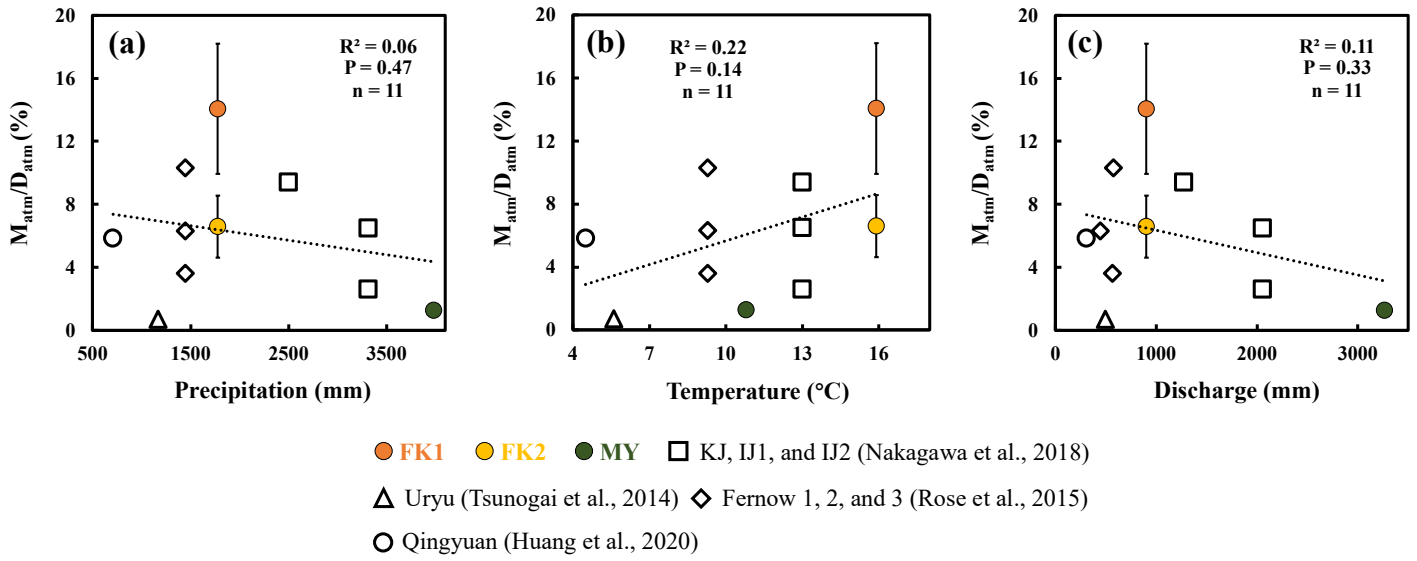
857 **Figure 4.** the M_{atm}/D_{atm} ratio plotted as a function of the amount of precipitation (a),

858 the M_{atm}/D_{atm} ratio plotted as a function of the temperature (b), and the M_{atm}/D_{atm} ratio

859 plotted as a function of flux of stream water (c) (FK1: orange circles; FK2: yellow

860 circles; MY: green circles). Those determined for the forested catchments in past studies

861 are plotted as well.

862

863

864

Figure 5. Schematic diagram showing the biogeochemical processing of nitrate in forested catchments under high precipitation (a) and low precipitation (b), where $NO_3^-{}_{atm}$ (unprocessed atmospheric nitrate) is represented by pink circles, $NO_3^-{}_{re}$ by yellow circles, the flows of $NO_3^-{}_{atm}$ by pink arrows, and those of $NO_3^-{}_{re}$ (remineralized nitrate) by yellow arrows (modified after Nakagawa., 2018). Although the deposition rates of $NO_3^-{}_{atm}$ (D_{atm}) and the biogeochemical reaction rates between (a) and (b) are the same, we can expect high $[NO_3^-]$ in (b). On the other hand, the M_{atm}/D_{atm} ratio between (a) and (b) are the same.